Franck-Condon factors via compressive sensing

Kevin Valson Jacob,[1,2] Eneet Kaur,[1,2] Wojciech Roga,[2] and Masahiro Takeoka[2]
[1]*Hearne Institute for Theoretical Physics and Department of Physics and Astronomy, Louisiana State University, Baton Rouge, Louisiana 70803, USA*
[2]*National Institute of Information and Communications Technology, Koganei, Tokyo 184-8795, Japan*

(Received 15 May 2020; accepted 6 July 2020; published 8 September 2020)

The probabilities of vibronic transitions in molecules are referred to as Franck-Condon factors (FCFs). Although several approaches for calculating FCFs have been developed, such calculations are still challenging. Recently it was shown that there exists a correspondence between the problem of calculating FCFs and boson sampling. However, if the output photon number distribution of boson sampling is sparse, then it can be classically simulated. Exploiting these results, we develop a method to approximately reconstruct the distribution of FCFs of certain molecules. We demonstrate its proof of concept by applying it to formic acid and thymine at 0 K. In our method, we first obtain the marginal photon number distributions for pairs of modes of a Gaussian state associated with the molecular transition. We then apply a compressive sensing method called polynomial-time matching pursuit to recover FCFs.

DOI: 10.1103/PhysRevA.102.032403

I. INTRODUCTION

In theoretical molecular spectroscopy, the goal is to obtain a better understanding of changes in molecular structure and the force field due to transitions by analyzing spectra of molecules. Of importance is the vibronic spectra of molecules, where the spectral lines correspond to transitions between two vibrational levels of electronic states. The probabilities of transitions between these levels are given by Franck-Condon factors (FCFs) which determine the intensities of the spectral lines. Given a vibronic spectrum, knowing which transitions contribute to observed spectral lines is helpful in testing a variety of molecules before synthesizing the most appropriate one for a particular application. Such applications include, for instance, increasing the efficiency of solar cells [1–3] or designing new organic light-emitting diodes (LEDs) [4]. Such organic LEDs could be used in display devices where narrow well-separated lines of specific frequencies are desired for the high-quality performance of the display. Therefore, it is relevant to develop algorithms to efficiently compute FCFs.

According to the Franck-Condon principle [5], the electronic levels of molecules are modeled as multimode quantum harmonic oscillators (HO). Therefore, the vibronic wave functions are multidimensional Hermite polynomials, and their overlaps are the transition probabilities (FCFs). Determining the vibronic spectra of molecules is challenging not only because of the fact that calculating the overlap of Hermite polynomials is computationally challenging [6] but also due to the exponential scaling of the number of possible vibronic transitions with the number of atoms of the molecule.

Franck-Condon factors in the harmonic approximation can be calculated using the exact iterative schemes [7,8]. The methods have been revised many times and several explicit formulas for specific factors have been derived. For instance, formulas for 141 FCFs with transitions with up to 11 excitations per mode have been discussed in Ref. [9]. Typically, a large number of FCFs are negligible, and applying direct methods makes computations inefficient. Therefore, different strategies of selecting the significant lines have been developed.

One such approximate strategy [10] involves using a simplified Duschinsky matrix by neglecting mode-mixing terms. A method based on block diagonalization of the Duschinsky matrix has been introduced in Ref. [11]. Restricting interest to a specific energy regime [12,13] or assuming that high occupation number configurations are negligible also leads to a reduction of the computational requirements [14–16]. Other methods rely on calculating spectra for a restricted number of excited modes, and on limiting the number of excitations per mode [17], where the parameters are chosen ad hoc. This can be done based on rigorous analysis which allows for estimating errors from such assumptions [18,19]. For the approaches based on the iterative methods, the indexing and searching of proper values preserved in the computational memory is one of the most important computational challenges [20]. A proposal to optimize this procedure has been given in Ref. [21]. Another approach to the approximate solutions is given by time-dependent algorithms. A time-dependent method was proposed in Ref. [22] for calculating the FCFs' density function as the Fourier transform of the overlap of an initial wave function and the wave function evolving over time. This approach has been developed further; for instance, see Refs. [23,24]. Parts of these algorithms for large molecules are designed for supercomputers and allow for finding billions of spectral lines. Moreover, alternative approaches to the problem of relating vibronic transitions and quantum simulations via boson sampling have been proposed as a potential application of quantum computing [25]. This problem has also been rephrased in terms of certain quantities in graph theory [26].

We propose the proof of concept of a method that is faster and requires less memory than the iterative methods [7,8].

However, this method deals with molecules with a highly sparse spectra. Roughly, we can say that our approach is appropriate for large molecules for which the number of significant lines of the spectra is linear with the number of modes. Although it is hard to predict in general which molecules have sparse spectra, we presume that molecules with rigid cores are likely to have this property. Some favorable features of our method are that it avoids memory problems and that required calculations are theoretically provably efficient. Moreover, as discussed in the Conclusions, our method's basic version presented here can be modified using more advanced computational techniques, thereby extending its applicability to a larger class of molecules.

In our method presented here, we apply compressive sensing [27–31] to approximately reconstruct the distribution of FCFs. Compressive sensing techniques, introduced in the seminal papers [27–31], are particularly useful for recovering sparse distributions from compressively sensed data. These techniques provide an efficient procedure to reconstruct a large but sparse dataset. In such techniques, compressively sensed data y are linearly related to a large unknown data set x via a measurement matrix A, i.e., $y = Ax$. Although this system of linear equations is underdetermined, owing to the sparsity of the data set to be reconstructed, various algorithms [27,32–37] for efficient recovery of x have been developed. These techniques have then been applied in various fields such as image reconstruction [38], communications [39], medical imaging [40], and quantum-state tomography [41].

In Ref. [42], following the work of Doktorov *et al.* [7], it was noted that there exists a parallel between molecular vibronic transitions and Gaussian boson sampling [43]. In this paradigm, it is possible to express the excited state as a Gaussian state [44], which is obtained by a Gaussian evolution of the ground state. FCFs can then be obtained as the probabilities of various photon number configurations of this excited state. However, finding the probabilities of various photon number distributions of a Gaussian state is known to be in the complexity class #P [26,45].

If the photon number distribution of the Gaussian state is sparse, then it is possible to recover this distribution approximately. This is possible by calculating the marginal photon number distributions over a few modes of the Gaussian state and then applying compressive sensing techniques to recover the full distribution. This idea was explored in Ref. [46]. The calculation of marginal photon number distributions over a few modes of the Gaussian states is computationally tractable. By employing a technique developed in Ref. [26], the probabilities of marginal photon number distributions can be calculated as loop Hafnians of certain matrices related to the Gaussian state (Sec. II B).

Our contribution is to develop a method to approximately reconstruct the distribution of FCFs. To this end, we apply *polynomial-time matching pursuit* (PTMP) [46] defined in Sec. II C. This is a first-order greedy algorithm that is a modification of the matching pursuit algorithm [32]. With this modification, the runtime of PTMP is polynomial in the number of modes of the excited Gaussian state. Since the number of modes is in general $3N_a - 6$, where N_a is the number of atoms of the molecule, PTMP is efficient when dealing with large molecules.

The key step of PTMP, which is also its computational bottleneck, is the identification of a column of the measurement matrix A which has the largest overlap with a specified vector in each iteration of the algorithm. This maximization procedure typically takes the time of the order of the size of the matrix A. However, if only the marginal photon number distributions of the nearest-neighbor modes are considered, then the problem can be mapped to an optimization in a one-dimensional (1D) Ising model [46]. The task is then to find the highest-energy configuration of a 1D classical spin chain with the Ising Hamiltonian that can be efficiently obtained.

In Sec. III, we demonstrate the feasibility of PTMP and analyze its performance in practice. We do this by approximately reconstructing the distributions of FCFs of two molecules: formic acid (7-mode symmetry block) in Sec. III A and thymine (26-mode symmetry block) in Sec. III B. In Sec. IV we discuss our method in comparison with other methods. Finally in the conclusions, Sec. V, we discuss the possible extensions of the technique.

II. METHODS

A. Gaussian transformation corresponding to a vibronic transition

Let us introduce a general formalism for describing bosonic Gaussian states [47,47–49]. We write the boson creation and annihilation operators for a given mode u as $\hat{a}_u^\dagger$ and $\hat{a}_u$, respectively, where we have the commutation relations $[\hat{a}_u, \hat{a}_v^\dagger] = \delta_{uv}$, where δ_{uv} is the Kronecker δ. For simplicity, we write the annihilation and creation operators of all the N modes as a vector of length $2N$ as

$$\vec{\hat{\zeta}} = (\hat{a}_1, \ldots, \hat{a}_N, \hat{a}_1^\dagger, \ldots, \hat{a}_N^\dagger) \tag{1}$$

$$\equiv (\hat{\zeta}_1, \hat{\zeta}_2 \ldots \hat{\zeta}_N, \hat{\zeta}_{N+1}, \ldots, \hat{\zeta}_{2N}). \tag{2}$$

A Gaussian state can be uniquely specified by its covariance matrix σ and its mean vector $\vec{\beta}$. In our convention, the covariance matrix corresponding to a state ρ is defined as

$$\sigma_{uv} = \frac{1}{2}\mathrm{Tr}[\rho\{\hat{\zeta}_u, \hat{\zeta}_v^\dagger\}] - \mathrm{Tr}[\rho\hat{\zeta}_u]\mathrm{Tr}[\rho\hat{\zeta}_v^\dagger], \tag{3}$$

where $\{\cdot,\cdot\}$ represents the anticommutator, and the mean vector is a column vector defined as

$$\vec{\beta} = \mathrm{Tr}[\rho\vec{\hat{\zeta}}\,]. \tag{4}$$

An electronic transition of a molecule defines a new set of vibrational modes which are displaced, distorted, and rotated with respect to the vibrational modes of the ground vibronic states. As the electronic excitation of the molecule may change forces between atoms as well as their mutual positions, the multimode HO corresponding to the excited state is usually expressed in a different coordinate system. If written in terms of normal coordinates, the change of the coordinate system is described by the linear relation [50]

$$q' = Uq + d, \tag{5}$$

where U is an orthogonal matrix referred to as the Duschinsky matrix, d is the displacement vector, and q and q' are the initial and final coordinates, respectively. These parameters may

be determined based on *ab initio* calculations of molecular structures [51].

In the Heisenberg picture, the transition between the two states can be expressed in terms of a transformation of the ladder operators of the multimode quantum harmonic oscillator. This transformation is a Bogoliubov transformation and is strictly related to the transformation of the normal coordinates given in Eq. (5). It was originally derived by Doktorov *et al.* [7] and was used recently to show the analogy between the vibronic molecular system and Gaussian boson sampling [42]. The transformation is

$$\hat{a}'^{\dagger} = \frac{1}{2}[J - (J^T)^{-1}]\hat{a} + \frac{1}{2}[J + (J^T)^{-1}]\hat{a}^{\dagger} + \frac{\vec{\delta}}{2} \tag{6}$$

$$\equiv \alpha\hat{a} + \beta\hat{a}^{\dagger} + \frac{\vec{\delta}}{2}, \tag{7}$$

with

$$J = \Omega' U \Omega^{-1}, \tag{8}$$

$$\vec{\delta} = \frac{\Omega' d}{\sqrt{\hbar}}, \tag{9}$$

$$\Omega' = \mathrm{diag}(\omega'_1, \ldots, \omega'_N)^{\frac{1}{2}}, \tag{10}$$

$$\Omega = \mathrm{diag}(\omega_1, \ldots, \omega_N)^{\frac{1}{2}}, \tag{11}$$

where U is the Duschinsky rotation matrix, d is the displacement vector from Eq. (5), and $\{\omega'_k\}$ and $\{\omega_k\}$ are the harmonic angular frequencies of the final and initial states, respectively. These variables are specified for a given molecule.

At any given temperature, the vibrational modes of the ground state of the molecule are in a thermal state ρ_i which is a Gaussian state. Since the evolution of the vibrational modes is specified by the Bogoliubov transformation in Eq. (6), the final state of the molecule ρ_f is also a Gaussian state. Therefore, we can apply the Gaussian formalism in order to find the covariance matrix and mean vector of the final Gaussian state. The evolution of the covariance matrix is given as

$$\sigma_f = S\sigma_i S^T, \tag{12}$$

where σ_f is the covariance matrix corresponding to the final state ρ_f, and σ_i is the covariance matrix corresponding to the initial state ρ_i. In our convention,

$$S = \begin{bmatrix} \alpha & \beta \\ \beta^* & \alpha^* \end{bmatrix},$$

where α and β are defined in Eq. (7). Since α and β are real, we can simplify the evolution of the covariance matrix as

$$\sigma_f = S\sigma_i S. \tag{13}$$

Let $\vec{d}_f$ be the mean vector corresponding to the state ρ_f, and let $\vec{d}_i$ be the mean vector corresponding to the state ρ_i. Then the mean vector evolves as

$$\vec{d}_f = S\vec{d}_i + \frac{\vec{\delta}}{\sqrt{2}}, \tag{14}$$

where $\vec{\delta}$ is defined in Eq. (9). In this work, we assume that the initial ground state is at 0 K and is thus a vacuum state. Therefore, the initial covariance matrix σ_i is the identity matrix, and the initial displacement d_i is a null vector. We then evolve the state according to Eq. (6) with the parameters specified by the molecule under consideration. Finally, Eqs. (13) and (14) completely specify the final state.

In order to obtain the photon number distribution of a few modes of a Gaussian state, we find the marginal state corresponding to the considered modes. This can be done by tracing over the irrelevant modes of the original Gaussian state. Alternatively, we can employ a simpler method to obtain the covariance matrix and the mean vector of the marginal state [52]. We obtain the covariance matrix of the marginal state by simply eliminating the rows and columns of the original state corresponding to the modes that are not considered. Similarly, we also obtain the mean vector of the marginal state.

The following subsection describes the procedure of obtaining the photon number distributions of these marginal states.

B. Photon number distributions of Gaussian states

A technique for calculating probabilities of photon distributions of a Gaussian state was developed in Refs. [26,45] and made concise in Ref. [53]. We now outline the method to calculate the probability of obtaining photon number distributions of a Gaussian state ρ with a covariance matrix σ and a mean vector $\vec{\beta}$. For notational simplicity, we define $\mathbf{X}$ as a $2N \times 2N$ block matrix:

$$\boldsymbol{X} = \begin{bmatrix} 0 & \mathbb{1}_N \\ \mathbb{1}_N & 0 \end{bmatrix}. \tag{15}$$

We also define $\boldsymbol{\sigma}_Q$ from the covariance matrix σ as

$$\boldsymbol{\sigma}_Q = \sigma + \frac{1}{2}\mathbb{1}_{2N}. \tag{16}$$

Following Ref. [53], we can then define

$$\boldsymbol{D} = \boldsymbol{X}\left(\mathbb{1}_{2N} - \boldsymbol{\sigma}_Q^{-1}\right), \tag{17}$$

$$\bar{\gamma}^T = \vec{\beta}^T \boldsymbol{\sigma}_Q^{-1}. \tag{18}$$

In order to obtain the probability of a photon number distribution $\vec{\boldsymbol{n}} = (n_1 \cdots n_N)$ from the Gaussian state characterized by σ and $\vec{\beta}$, we have the following steps.

(i) Calculate matrix $\boldsymbol{B}$ as follows: For each $i = 1, 2, \ldots, N$, the ith row as well as the $(N+i)$th row of $\boldsymbol{D}$ are repeated n_i times, and the ith column as well as the $(N+i)$th column of $\boldsymbol{D}$ are repeated n_i times. The resulting matrix $\boldsymbol{B}$ is a $2\bar{n}$-dimensional square matrix, where $\bar{n} = \sum n_i$.

(ii) Define a vector $\bar{\gamma}$ of length $\bar{n}$ as follows: For each $i = 1, 2, \ldots, N$, the ith element as well as $(N+i)$th element of γ is repeated n_i times.

(iii) Replace the diagonal entries of $\boldsymbol{B}$ with $\bar{\gamma}$ so as to obtain a matrix $\boldsymbol{C}$.

The probability of obtaining a photon distribution $\vec{\boldsymbol{n}}$ is then

$$\mathrm{Prob}(\vec{\boldsymbol{n}})_\rho = F \times \mathrm{lhaf}(\boldsymbol{C}), \tag{19}$$

where

$$F = \frac{\exp\left(-\frac{1}{2}\vec{\beta}^{\dagger}\boldsymbol{\sigma}_Q^{-1}\vec{\beta}\right)}{\sqrt{\det(\boldsymbol{\sigma}_Q)}\prod_{i=1}^{N} n_i!}, \tag{20}$$

and the function lhaf is the loop Hafnian defined as

$$\mathrm{lhaf}(G) = \sum_{M\in W}\prod_{(i,j)\in M} G_{ij}, \tag{21}$$

where W is the set of all the perfect matchings of a graph G with loops. A detailed example of this construction is shown in Appendix A. In this work, loop Hafnians were obtained by using an algorithm from Ref. [54].

Calculating loop Hafnians of large matrices is not efficient [26]. However, as can be observed, $\boldsymbol{C}$ has several repeated columns and rows. In such cases, one can also use a tailored formula for structured matrices, as given in Ref. [55], which allows a faster calculation of loop Hafnians.

The method outlined above is not defined when we are interested in finding the probability of obtaining vacuum in the final Gaussian state. This is because the above procedure produces a zero-dimensional matrix $\boldsymbol{C}$. Fortunately, the vacuum probability is the overlap of two Gaussian states for which there is an efficient formula [56]. For an N-mode Gaussian state ρ with a covariance matrix σ and a mean vector $\vec{\beta}$, the overlap with vacuum is given as

$$\mathrm{Tr}[\rho|\mathbf{0}\rangle\langle\mathbf{0}|] = \frac{\exp\left[-\frac{1}{2}\vec{\beta}^T\left(\sigma+\frac{1}{2}\mathbb{1}_{2N}\right)^{-1}\vec{\beta}\right]}{\sqrt{\det\left(\sigma+\frac{1}{2}\mathbb{1}_{2N}\right)}}. \tag{22}$$

This result could also have been obtained from Eq. (19) by defining loop Hafnians of zero-dimensional matrices as one.

In our approach, we restrict ourselves to two-mode Gaussian states and limit the number of photons to three photons per mode. This makes the calculation of loop Hafnians easily tractable with an ordinary desktop computer and is sufficient for the examples of molecules we consider. The restriction of calculations to two modes and up to three photons per mode was a pragmatic choice and not a fundamental limitation of the method. We observe that for molecules discussed in Sec. III, the probabilities of transitions with occupation numbers higher than 3 are negligible. We have tested the computational time needed to calculate the marginal distributions for two modes and up to six photons per mode. The computational time on a standard processor of a desktop computer was around 100 s. The marginal distributions with higher occupation numbers could be computed in reasonable time by more powerful machines. Testing this is however out of the scope of our proof of concept demonstration. The restriction to two neighboring modes is also not a fundamental limitation. The algorithm described in the next section can be easily adapted to deal with three or more neighboring modes in polynomial time.

C. Polynomial-time matching pursuit

Polynomial-time matching pursuit (PTMP) is a modification of the standard matching pursuit iterative algorithm [32] developed in the context of compressive sensing for finding a sparse high-dimensional signal x that fits a given low-dimensional measurement data y. The transformation from x to y is given by a known rectangular measurement matrix A, i.e., $y = Ax$. In the case under consideration x is the vector of FCFs, and y is a vector of marginal photon number distributions. Then, A is defined as in Ref. [46]. For completeness, we provide the exact form of A in Appendix B.

PTMP is applicable when y consists of nearest-neighbor marginal distributions. The algorithm is as follows.

(i) Initialization: Define residue $r^0 = y$ and the reconstructed vector x^0 as the zero vector.

(ii) Support detection: In step i, find the index t of the column of A with the maximum overlap with the residue r^{i-1}, i.e., $t = \arg\max_{t'}(A^T r^{i-1})_{t'}$.

(iii) Updating: Update the residue as $r^i = r^{i-1} - sA_t$, where s is a chosen step size and A_t is a column of A detected in the previous step. Also, update the tth entry of the reconstructed vector as $x_t^i = x_t^{i-1} + s$.

We continue the iteration until a stopping criterion is met. For us, this criterion is when the elements of x sum up to 1. This ensures that the sum of the transition probabilities is equal to 1. We note that this modification of matching pursuit relies on the non-negativity of the vectors and the matrices involved. However, the procedure is easily adaptable to the general case.

The bottleneck of this algorithm is the support detection part. Fortunately, when we consider only marginal states of neighboring modes m and $m+1$, $A^T r$ has the structure

$$[\mathbf{1}^{\otimes m-1}\otimes(r_{0_m,0_{m+1}}, r_{0_m,1_{m+1}}, r_{0_m,2_{m+1}},\ldots)\otimes\mathbf{1}^{\otimes N-m-1}]^T, \tag{23}$$

where N is the total number of modes and $r_{n_m,n'_{m+1}}$ denotes the probability of having n photons in the mth mode and n' photons in the $(m+1)$th mode. Here, $\mathbf{1}^{\otimes l}$ is a vector of length K^l with all entries 1, where $K-1$ is the maximum number of photons in a mode. So, $A^T r$ for all pairs of neighboring modes is the sum of terms (23) and has the structure of the nearest-neighbor interaction Hamiltonian for 1D spin chains [57].

The configuration of spins that maximizes the energy of this system, and thereby the index of the maximum entry of vector $A^T r$, can be found efficiently using the following iterative algorithm [58]:

$$\begin{aligned} &E_1(i_1) = 0,\\ &E_k(i_k) = \max[E_{k-1}(i_{k-1}) + H_{k-1,k}(i_{k-1}, i_k)], \quad k \geqslant 2, \end{aligned} \tag{24}$$

where matrix $H_{k-1,k}$ with the two arguments i_{k-1} and i_k is defined by

$$H_{k-1,k}(i_{k-1}, i_k) = r_{(i-1)_{k-1},(i-1)_k}. \tag{25}$$

In the original algorithm, $E_k(i_k)$ is the optimized energy of spins $1,\ldots,k$ assuming that spin k is in state i_k. In each step, for each column (i_k) the maximization in Eq. (24) allows us to find the index of the maximum entry in this column. This index would indicate the state of $k-1$ spins if the kth spin was found in state i_k in the final solution. In each iteration, for each state of the currently considered spin, we have a unique sequence of states of previous spins that maximizes the energy. The final maximization determines the correct sequence of states of the entire spin chain. This enables us to find the index of the maximum entry of the vector $A^T r$. The efficiency of PTMP follows from the ability to efficiently find

the maximum-energy configuration of a classical spin chain in 1D.

This procedure allows us to efficiently find the approximate distribution of sparse FCFs of molecules from the photon number distributions of nearest-neighbor marginals. By sparse FCFs, we mean that either only a few FCFs are nonzero or that just a few FCFs are significantly higher than the rest.

III. RESULTS: SIMULATION OF FC FACTORS

We now demonstrate the algorithm described in Sec. II C for formic acid and thymine.

A. Formic acid

As an example, let us consider formic acid. In particular, we analyze its 7-mode symmetry block with the normal-mode wave numbers

$$(3629.9; 3064.9; 1566.5; 1399.7; 1215.3; 1190.9; 496.3)\ (\mathrm{cm}^{-1}) \tag{26}$$

for the electronic transition $(1^1A'') \rightarrow (1^2A')$. The parameters defining this transition are given in Ref. [42].

We obtain the marginal probabilities of photon numbers in adjacent modes, considering up to three photons per mode. This result was then used to reconstruct the distribution of FCFs using PTMP. We emphasize that restricting the marginal distributions to two neighboring modes does not imply that our method will miss simultaneous transitions involving more than two modes. The marginal measurements give us only constraints for the joint distribution. If there exists a global solution with simultaneous transitions that involves more than two modes and that still fits all marginal distributions, it will be taken into account by our method. The step size in our algorithm is chosen as $s = 0.01$, which necessitates no more than $k = 100$ iterations of our algorithm. Also, we do not need to change the parameters s and k for larger molecules.

As we consider a small molecule and limit the maximum number of photons per mode, the exact approach by Doktorov *et al.* [7] is computationally tractable using a standard desktop computer. This enables us to plot the result of the reconstruction by PTMP together with the exact spectrum in Fig. 1. As a reconstruction quality measure, we use the $l1$-norm between the exact FCFs (p) and the reconstructed FCFs (q) defined as $D_{\mathrm{tr}} = \sum_i |p_i - q_i|$. For two positive vectors normalized to one, this measure can vary between 0 for identical vectors and 2 for vectors with nonoverlapping supports.

The main lines shown in Fig. 1 are described in Table I. We observe that the main lines correspond to one, two, and three photons excited in a particular mode. Our reconstruction also allows us to recognize lines corresponding to simultaneous excitation in two different modes. In our method we did not assume *a priori* that the total number of excitations per mode should be small or that only a few modes are excited at once.

Notice that the numbers Table I do not sum up to 1. The reason is that we have stopped iterating when we started recording contributions for peak 0. We know that this is an error, as this peak was calculated exactly via Gaussian overlaps, and its contribution from the residue was removed.

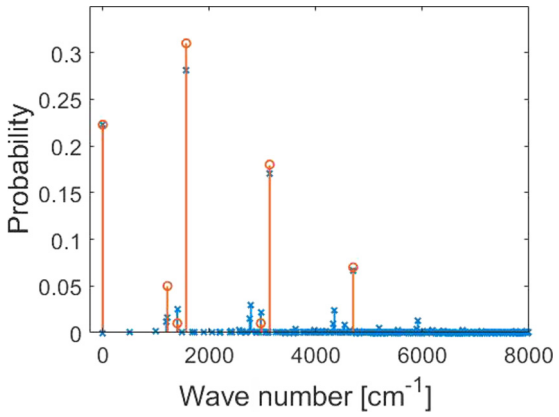

FIG. 1. Franck-Condon factors for transitions between the electronic ground state $(1^1A'')$ and the vibrational states in the electronic excited state $(1^2A')$ of formic acid at 0 K. The blue lines with crosses represent the spectrum obtained by the exact Doktorov recursive method, the orange lines with circles represent the spectrum reconstructed from the nearest-neighbors' marginal distributions by PTMP. The reconstruction quality (the $l1$-norm between the reconstructed distribution and the exact one) is 0.2991.

Further iterations will produce false results. We estimate that lines of the total probability weight of about 0.147 are not recognized by the method.

Since formic acid is small enough that its FCFs can be reconstructed by other methods, we compare the performance of PTMP with another compressive sensing method. This method finds a solution which fits the marginal distributions while minimizing its $l1$-norm. For this, we use the constrained $l1$-norm minimization in MATLAB using the CVX package [59]. The spectrum thus obtained is plotted in Fig. 2.

From Figs. 1 and 2, we infer that the quality of the reconstruction is more accurate while using norm minimization (0.1988) than while using PTMP (0.2911). It is known that norm minimization provides more accurate solutions than first-order iterative algorithms like matching pursuit (see, for instance, Ref. [36]). However, norm minimization requires more memory than first-order iterative algorithms. Furthermore, the former scales badly with the size of the problem. In particular, it is inefficient for finding the distribution of FCFs of thymine which we consider next. In contrast, PTMP does not experience computational time or memory problems.

TABLE I. Main FCFs of formic acid reconstructed from marginal distributions of photon numbers in the nearest-neighbor modes by PTMP. The modes correspond to the symmetry block with seven normal modes with wave numbers in Eq. (26).

Wave number (cm^{-1})	Photon number state	Probability
0	0000000	0.2228
1566.5	0010000	0.31
3132.9	0020000	0.18
4699.4	0030000	0.07
1215.3	0000100	0.05
1399.7	0001000	0.01
2966.1	0011000	0.01

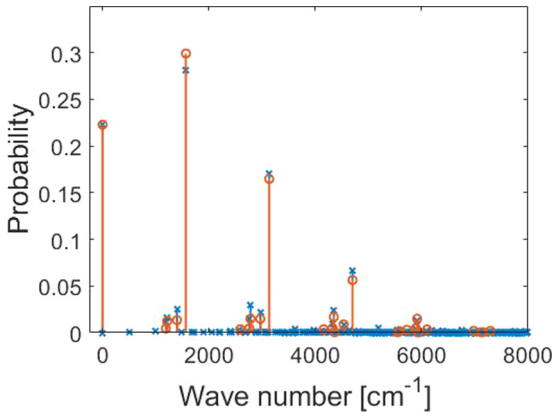

FIG. 2. Franck-Condon factors for transitions between the electronic ground state ($1^1A''$) and the vibrational states in the electronic excited state ($1^2A'$) of formic acid at 0 K. The blue lines with crosses represent the spectrum obtained by the exact Doktorov recursive method, the orange lines with circles represent the spectrum of the minimum $l1$-norm that fits the nearest-neighbors' marginal distributions. The reconstruction quality (the $l1$-norm between the reconstructed distribution and the exact one) is 0.1988.

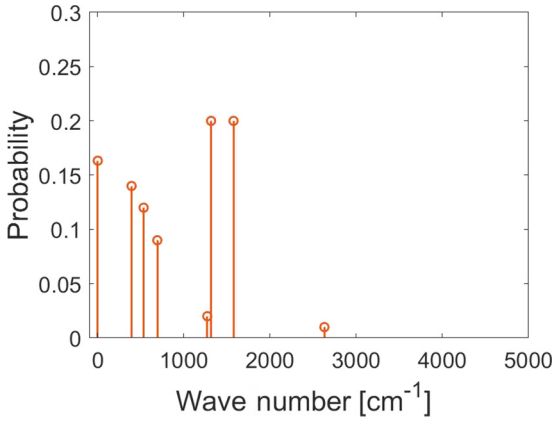

FIG. 3. Franck-Condon factors for transitions between the electronic ground state ($1^1A''$) in 0 K and 26 vibrational modes of an excited electronic state ($1^2A'$) of thymine. This spectrum is recovered by PTMP from marginal distributions for all nearest-neighbor modes.

B. Thymine

As the second example we consider thymine. Its vibrational degrees of freedom can be decoupled into two separate blocks of 13 normal modes and 26 normal modes. We consider the transitions at 0 K between the ground electronic state ($1^1A''$) and 26 vibrational modes of the excited state ($1^2A'$) with normal wave numbers as follows:

$$(3535.0; 3511.8; 3195.7; 3150.6; 2996.8; 1833.9; 1739.7;$$
$$1575.5; 1531.1; 1474.4; 1442.6; 1380.0; 1353.8; 1315.0;$$
$$1271.3; 1216.1; 1187.3; 995.9; 893.5; 766.6; 690.7; 581.6;$$
$$532.2; 444.4; 392.2; 293.8)\ (\mathrm{cm}^{-1}). \quad (27)$$

Obtaining the spectrum of thymine is more challenging with standard techniques. This is because, even if we restrict ourselves to transitions with no more than three photons per mode, then the number of all possible FCFs is 4^{26}. Therefore, dealing with this molecule using standard methods such as the exact recursive Doktorov method is infeasible on standard desktop computers. Also, the $l1$-norm minimizer cannot deal with problems of this size.

Based on the parameters of the transition provided in Refs. [18,25], we obtain the Gaussian state associated with the excited state of the transition. Next, we find the marginal states for nearest-neighbor modes and then find their photon number distributions up to three photons per mode. Finally, we apply the PTMP algorithm to find the FCFs. We show the spectrum of FCFs of thymine in Fig. 3 and in Table II.

The approximate spectrum of FCFs of thymine produced by PTMP agrees well with the spectra produced by other methods [18]. Although our method is not as precise as the method given in Ref. [18], the computation time is faster. In particular, the calculations used to produce the spectrum given in Fig. 3 take only a few seconds on a standard desktop computer. We observe that in thymine single-photon transitions in different modes dominate, unlike in the case of formic acid.

Let us comment on the sparsity assumption for our method. Although the exact spectrum of FCFs of thymine is not sparse [18,42], there are six lines with probabilities significantly higher than those of the other lines of the spectrum. This situation is similar to a sparse signal in the presence of noise. We observe that even though many small probability contributions are present, we are still able to reconstruct the most significant lines of the spectrum. This shows that our algorithm does not demand strict sparsity of FCFs. However, recognizing the lines with lower probabilities is out of the reach and beyond the scope of this approach.

IV. COMPARISON TO OTHER APPROXIMATING METHODS

Although our method is not designed to be a tool competing with the advanced methods of high-precision vibronic spectroscopy, it can be used as a computational time- and memory-efficient approximate method for estimating the main spectral lines, and as such it can support the more precise and computationally expensive tools. Aside from the fact that our method is time and memory efficient, it has some advantages over the existing approximate methods as described below.

TABLE II. Main FCFs of thymine reconstructed from marginal distributions of photon numbers in the nearest-neighbor modes by PTMP. The modes correspond to the symmetry block with 26 normal modes with wave numbers in Eq. (27).

Wave number (cm^{-1})	Photon number state	Probability
0	0 photon in all modes	0.1633
392.2	1 photon in 25th mode	0.14
532.2	1 photon in 23rd mode	0.12
690.7	1 photon in 21st mode	0.09
1315.0	1 photon in 14th mode	0.2
1575.5	1 photon in 8th mode	0.2

For formic acid, we notice that the positions of the largest lines correspond to either 0 or the frequency (or its multiplicities) associated with the largest displacement. For thymine it is similar, although we do not detect multiplicities. If we approximate the Duschinsky matrix as in Ref. [11], then we can divide the problem into separate blocks that can be treated separately. In this way, some rough information about the spectrum can be taken just from the approximate Duschinsky matrix and the displacement vector. However, we notice several advantages that our method may provide. First of all, the marginal distributions in our approach can be known exactly with relatively minimal effort. To the best of our knowledge, this is something that neither exact methods [7,8] nor approximate methods [10,22] offer without first calculating the full spectra.

Second, our method allows for estimating which part of the spectrum has been actually found. This is because we can see which part of the detected spectrum covers the marginal distributions which are exact. So, our method is not just guessing where the main lines are, but allowing us to estimate the total mass of the lines that we do not observe, albeit roughly. This is something one does not see if approximate Duschinsky matrix and displacement vectors are used. However, precise estimation of the mass of undetected lines needs further investigation.

It does not seem obvious when multiplicities of the frequencies play an important role or not. This question is related to prescreening procedures [18]. A third advantage of our method is that it allows us to test with relative ease whether transitions involving higher quantum numbers are significant or not, as this can be readily observed from the marginal distributions.

Fourth, our method predicts the exact position of the main lines. With the time-dependent methods [22–24], the approximate density distributions may be characterized only with a small resolution; i.e., lines close to each other may be indistinguishable. In contrast, our method, which shows the precise positions of main lines, covers complementary features of the approximate spectrum.

The final argument in favor of our method is its potential to be extended. Several other methods can be applied to get more accurate reconstructions from the exact constraints. A few such extensions are sketched in Sec. V.

V. CONCLUSIONS

In this paper, we provide the proof of concept of an efficient classical method to approximately reconstruct the distribution of FCFs of large molecules. This reconstruction is possible with an efficient compressive sensing algorithm that uses marginal photon number probability distributions as compressively sensed data. We define and test the performance of the PTMP algorithm that allows us to efficiently reconstruct the main peaks of molecular vibronic spectra even for large molecules.

Our method is restricted to spectra which are sparse or spectra with just a few FCFs significantly larger than the rest. In the case of decreasing sparsity, we would need more marginal distributions to reliably reconstruct significant FCFs. In such a case, instead of two nearest-neighbor modes, we can consider three or more nearest-neighbor modes. PTMP can be easily adapted and is efficient for this case. However, the computational time for calculating loop Hafnians increases exponentially with the number of modes that restrict the method.

An alternative way of extending the method is to use a marginal distribution from not necessarily nearest-neighbor modes. In this case, PTMP cannot be used to find the largest element in a vector in the support detection scheme in the presented form. This task would be mapped on the Ising problem with non-nearest-neighbor interactions—a more general spin-glass problem. In full generality, this is a challenge that belongs to the complexity class NP-complete and is mapped to the max-cut problem in graph theory [60]. However, for special types of graphs called planar graphs, there exists a polynomial-time algorithm [61,62]. We could use these algorithms for support detection with constraints from marginal distributions involving not necessarily nearest-neighbor modes. The method can be extended even further when more advanced computational techniques that can deal with Ising models with nonlocal interactions are used. As instances of such techniques, we may consider the quantum Monte Carlo approach or quantum annealing. These techniques show that the method we propose can be strongly extended and have the potential to deal more accurately with more complicated problems.

Since we study FCFs at temperature 0 K, we can assume that each mode of the final state is occupied by only a few photons. However, when the temperature is finite, the initial state of the molecule is a thermal state with the average number of photons per mode obeying the Bose-Einstein distribution. If the number of photons per mode is high, then the marginal distributions containing relatively few photons are improbable. In such cases, although we have to calculate loop Hafnians of large matrices, these matrices are highly structured with only a few dissimilar rows or columns. Then, we can employ the method of Kan [55] to calculate such loop Hafnians. This is a subject for future studies.

Finally, the method of FCFs recovered from marginal distributions by compressive sensing may be improved by introducing algorithms other than PTMP. This can include gradient pursuit introduced in Ref. [34] as discussed in Ref. [46]. We also think that orthogonal matching pursuit [37] can be adapted for this purpose.

ACKNOWLEDGMENTS

The authors are grateful to Jonathan P. Dowling for initiating the collaboration between Louisiana State University, USA, and the National Institute of Information and Communications Technology, Japan, that led to multiple research works including this work. His insight and guidance will be immensely missed. The authors thank Joonsuk Huh for sharing the Duschinsky matrix for thymine. The authors also thank Gao Qi and Takafumi Ono for helpful discussions. K.V.J. acknowledges the support from the NSF and from the Louisiana State University System Board of Regents via an Economic Development Assistantship. E.K. acknowledges support from the U.S. Office of Naval Research. W.R. and

M.T. acknowledge the support of JST CREST Grant No. JPMJCR1772.

APPENDIX A: PHOTON NUMBER DISTRIBUTIONS OF A GAUSSIAN STATE

As an example of calculating the photon number distribution of a multimode Gaussian state, consider a two-mode Gaussian state described by a covariance matrix σ and a mean vector β as follows:

$$\sigma = \begin{bmatrix} \sigma_{11} & \sigma_{12} & \sigma_{13} & \sigma_{14} \\ \sigma_{21} & \sigma_{22} & \sigma_{23} & \sigma_{24} \\ \sigma_{31} & \sigma_{32} & \sigma_{33} & \sigma_{34} \\ \sigma_{41} & \sigma_{42} & \sigma_{43} & \sigma_{44} \end{bmatrix}, \tag{A1}$$

$$\vec{\beta} = \begin{bmatrix} \beta_1 & \beta_2 & \beta_3 & \beta_4 \end{bmatrix}^T. \tag{A2}$$

We are interested in the probability of obtaining two photons in mode 1 and one photon in mode 2. We first calculate the matrix $\boldsymbol{D}$ as in Eq. (17). Then we construct the 6×6 matrix $\boldsymbol{B}$ as

$$\boldsymbol{B} = \begin{bmatrix} D_{11} & D_{11} & D_{12} & D_{13} & D_{13} & D_{14} \\ D_{11} & D_{11} & D_{12} & D_{13} & D_{13} & D_{14} \\ D_{21} & D_{21} & D_{22} & D_{23} & D_{23} & D_{24} \\ D_{31} & D_{31} & D_{32} & D_{33} & D_{33} & D_{34} \\ D_{31} & D_{31} & D_{32} & D_{33} & D_{33} & D_{34} \\ D_{41} & D_{41} & D_{42} & D_{43} & D_{43} & D_{44} \end{bmatrix}. \tag{A3}$$

Constructing $\vec{\gamma}$ as per Eq. (18), we obtain

$$\bar{\gamma} = \begin{bmatrix} \gamma_1 & \gamma_1 & \gamma_2 & \gamma_3 & \gamma_3 & \gamma_4 \end{bmatrix}^T. \tag{A4}$$

Next, we replace the diagonal entries of $\boldsymbol{B}$ with $\bar{\gamma}$ so as to obtain

$$\boldsymbol{C} = \begin{bmatrix} \gamma_1 & D_{11} & D_{12} & D_{13} & D_{13} & D_{14} \\ D_{11} & \gamma_1 & D_{12} & D_{13} & D_{13} & D_{14} \\ D_{21} & D_{21} & \gamma_2 & D_{23} & D_{23} & D_{24} \\ D_{31} & D_{31} & D_{32} & \gamma_3 & D_{33} & D_{34} \\ D_{31} & D_{31} & D_{32} & D_{33} & \gamma_3 & D_{34} \\ D_{41} & D_{41} & D_{42} & D_{43} & D_{43} & \gamma_4 \end{bmatrix}. \tag{A5}$$

Finally, the loop Hafnian of the above matrix is calculated and then used to calculate the concerned probability using Eq. (19).

We now demonstrate this technique. Consider a two-mode coherent state $\rho = |\lambda, \zeta\rangle\langle\lambda, \zeta|$. The covariance matrix and the mean vector corresponding to this state as defined in Eqs. (3) and (4) are

$$\sigma = \frac{\mathbb{1}_4}{2}, \tag{A6}$$

$$\vec{\beta} = \begin{bmatrix} \lambda & \zeta & \lambda^* & \zeta^* \end{bmatrix}^T. \tag{A7}$$

For this state, $\boldsymbol{\sigma}_Q$ as defined in Eq. (16) is identity, and hence $\boldsymbol{D}$ as defined in Eq. (17) as well as $\boldsymbol{B}$ defined subsequently are zero. These simplify our calculations.

Since $\boldsymbol{\sigma}_Q = \mathbb{1}_4$, we then find from Eq. (18) that $\vec{\gamma} = \vec{\beta}$. Thus we obtain

$$\bar{\gamma} = [\lambda \quad \lambda \quad \zeta \quad \lambda^* \quad \lambda^* \quad \zeta^*]^T. \tag{A8}$$

We then construct the matrix $\boldsymbol{C}$. We observe that it is a diagonal matrix with its diagonal as $\bar{\gamma}$. Using the fact that the loop Hafnian of a diagonal matrix is just the product of the diagonal terms, we obtain its loop Hafnian as $|\lambda|^4|\zeta|^2$.

A prefactor needed in our final expression is then calculated from Eq. (20) as

$$F = \frac{\exp(-|\lambda|^2 - |\zeta|^2)}{2!}. \tag{A9}$$

Finally, using Eq. (19) we obtain the probability of obtaining two photons in mode 1 and one photon in mode 2 as

$$\text{Prob}(2, 1)_{|\lambda,\zeta\rangle} = \exp(-|\lambda|^2 - |\zeta|^2)\frac{|\lambda|^4|\zeta|^2}{2!}. \tag{A10}$$

This expression can easily be verified as obeying the Poissonian distribution of coherent states.

APPENDIX B: MEASUREMENT MATRIX

Since our measurement matrix is large, it is imperative that we develop a particular representation of the measurement matrix such that its elements can be efficiently generated by knowing its indices alone. This makes our algorithm efficient with respect to its memory requirement.

In order to define the measurement matrix, we first develop a representation for the vector (x) with all FCFs. To this end, we define vectors specified by sets of photon numbers in each mode $\{n_1, n_2, \ldots\}$, where n_i denotes the number of photons in the ith mode as follows:

$$|n_1, n_2, \ldots\rangle^T = \underset{\substack{\uparrow \\ n_1+1}}{(\cdots 1 \cdots)} \otimes \underset{\substack{\uparrow \\ n_2+1}}{(\cdots 1 \cdots)} \otimes \underset{\cdots}{\cdots}. \tag{B1}$$

Here the lower indices indicate the positions of 1 in each component of the tensor product, and the remaining entries are zeros. Using this representation, we can then decompose the vector x of all FCFs of an N-mode system as follows:

$$x = \sum_{n_1,\ldots,n_N} \alpha_{n_1,\ldots,n_M} |n_1, \ldots, n_N\rangle. \tag{B2}$$

Here, the coefficients $\alpha_{n_1,\ldots,n_N}$ are non-negative and sum up to 1.

We now show how to define the measurement matrix in this representation. For this, let us first define the following auxiliary vectors:

$$\gamma_{n_i} = \mathbf{1}^{\otimes i-1} \otimes \underset{\substack{\uparrow \\ n_i+1}}{(\cdots 1 \cdots)} \otimes \mathbf{1}^{\otimes N-i}. \tag{B3}$$

where $\mathbf{1} = (1, 1, 1, \ldots)$ and $(\cdots 1 \cdots)$ are K-dimensional vectors and $K - 1$ is the maximum photon number in a mode. γ_{n_i} is defined such that $\gamma_{n_i} x$ gives the marginal probability of having n_i photons in the ith mode. By choosing different n_i, we can then obtain the marginal probability distribution of the photon numbers in mode i.

FIG. 4. Depiction of the first 600 columns of the $96 \times 16\,384$ measurement matrix that we used for formic acid. White denotes the value 1 and black denotes 0. We considered nearest-neighbor marginals of the 7-mode symmetry block with up to three photons per mode.

In order to find the marginal distributions of two modes, we use the entrywise products $\gamma_{n_i} \odot \gamma_{n_j}$ such that $(\gamma_{n_i} \odot \gamma_{n_j})x$ is just the marginal probability of simultaneously finding n_i photons in the ith mode and n_j photons in the jth mode. These quantities allow us to write the marginal distributions of photonic occupations in pairs of modes.

In the problem that we are concerned, the measurement matrix A consists of rows indexed by (n_i, n_j) given as

$$A_{n_i,n_j} = \gamma_{n_i} \odot \gamma_{n_j}. \tag{B4}$$

This matrix describes the transition from the joint distribution of FCFs for all modes and marginal distributions for pairs of modes. Using this form of the measurement matrix, the vector of joint marginal distributions (y) is given as

$$y_{n_i,n_j} = A_{n_i,n_j}x. \tag{B5}$$

We can now apply compressive sensing methods to our problem. A representation of the measurement matrix that we used for formic acid is shown in Fig. 4.

[1] J. Hachmann, R. Olivares-Amaya, S. Atahan-Evrenk, C. Amador-Bedolla, R. S. Sánchez-Carrera, A. Gold-Parker, L. Vogt, A. M. Brockway, and A. Aspru-Guzik, J. Phys. Chem. Lett. **2**, 2241 (2011).

[2] H. J. Butler, B. B. L. Ashton, G. Cinque, K. Curtis, J. Dorney, K. Esmonde-White, N. J. Fullwood, B. Gardner, P. L. Martin-Hirsch, M. J. Walsh, M. R. McAinsh, N. Stone, and F. L. Martin, Nat. Protoc. **11**, 664 (2016).

[3] M. Gross, D. C. Müller, H.-G. Nothofer, U. Scherf, D. Neher, C. Bräuchle, and K. Meerholz, Nature (London) **405**, 661 (2000).

[4] A. F. Rausch, M. E. Thompson, and H. Yersin, Chem. Phys. Lett. **468**, 46 (2009).

[5] V. P. Gupta, *Principles and Applications of Quantum Chemistry* (Academic, San Diego, 2016), pp. 313–318.

[6] D. S. Phillips, M. Walschaers, J. J. Renema, I. A. Walmsley, N. Treps, and J. Sperling, Phys. Rev. A **99**, 023836 (2019).

[7] E. V. Doktorov, I. A. Malkin, and V. I. Mańko, J. Mol. Spectrosc. **64**, 302 (1977).

[8] T. E. Sharp and H. M. Rosenstock, J. Chem. Phys. **41**, 3453 (1964).

[9] J. Weber and G. Hohlneicher, Mol. Phys. **101**, 2125 (2003).

[10] K. M. Ervin, T. M. Ramond, G. E. Davico, R. L. Schwartz, S. M. Casey, and W. C. Lineberger, J. Phys. Chem. A **105**, 10822 (2001).

[11] A. Toniolo and M. Persico, J. Comput. Chem. **22**, 968 (2001).

[12] R. Berger, C. Fischer, and M. Klessinger, J. Phys. Chem. A **102**, 7157 (1998).

[13] M. Dierksen and S. Grimme, J. Phys. Chem. A **108**, 10225 (2004).

[14] V. I. Baranov, L. A. Gribov, and B. K. Novosadov, J. Mol. Struct. **70**, 1 (1981).

[15] D. Kohn, E. J. Robles, C. Logan, and P. Chen, J. Phys. Chem. **97**, 4936 (1993).

[16] P. Ruhoff and M. Ratner, Int. J. Quantum Chem. **77**, 383 (2000).

[17] F. Santoro, J. Chem. Phys. **126**, 084509 (2007).

[18] H.-C. Jankowiak, J. L. Stuber, and R. Berger, J. Chem. Phys. **127**, 234101 (2007).

[19] M. Islampour, R. Dehestani, and S. H. Lin, Mol. Spectrosc. **194**, 179 (1999).

[20] D. Gruner and P. Brumer, J. Chem. Phys. **138**, 310 (1987).

[21] S. M. Rabidoux, V. Eijkhout, and J. F. Stanton, J. Chem. Theory Comput. **12**, 728 (2016).

[22] E. J. Heller, Acc. Chem. Res. **14**, 368 (1981).

[23] A. Baiardi, J. Bloino, and V. Barone, J. Chem. Theory Comput. **9**, 4097 (2013).

[24] J. Huh and R. Berger, Faraday Discuss. **150**, 363 (2011).

[25] J. Huh and M.-H. Yung, Sci. Rep. **7**, 7462 (2017).

[26] N. Quesada, J. Chem. Phys. **150**, 164113 (2019).

[27] E. J. Candes and T. Tao, IEEE Trans. Inf. Theory **51**, 4203 (2005).

[28] D. L. Donoho, Commun. Pure Appl. Math. **59**, 907 (2006)

[29] E. J. Candes and T. Tao, IEEE Trans. Inf. Theory **52**, 5406 (2006).

[30] R. Baraniuk, M. Davenport, R. DeVore, and M. Wakin, Constr. Approx. **28**, 253 (2008).

[31] E. J. Candes, J. Romberg, and T. Tao, IEEE Trans. Inf. Theory **52**, 489 (2006).

[32] S. G. Mallat and Z. Zhang, IEEE Trans. Signal Process. **41**, 3397 (1993).

[33] G. Davis, S. Mallat, and M. Avellaneda, Constr. Approx. **13**, 57 (1997).

[34] T. Blumensath and M. E. Davies, IEEE Trans. Signal Process. **56**, 2370 (2008).

[35] T. Blumensath and M. E. Davies, J. Fourier Anal. Appl. **14**, 629 (2008).

[36] A. Draganic, I. Orovic, and S. Stankovic, Facta Univ., Ser.: Electron. Energ. **30**, 477 (2017).

[37] T. Zhang, IEEE Trans. Inf. Theory **57**, 6215 (2011).

[38] J. Romberg, IEEE Signal Process. Mag. **25**, 14 (2008).

[39] R. Mihajlovic, M. Scekic, A. Draganic, and S. Stankovic, in *Proceeding of the 3rd Mediterranean Conference on Embedded Computing, MECO 2014, Budva, Montenegro* (IEEE, 2014).

[40] M. Lustig, D. Donoho, and J. M. Pauly, Magn. Reson. Med. **58**, 1182 (2007).

[41] D. Gross, Y.-K. Liu, S. T. Flammia, S. Becker, and J. Eisert, Phys. Rev. Lett. **105**, 150401 (2010).

[42] J. Huh, G. G. Guerreschi, B. Peropadre, J. R. McClean, and A. Aspuru-Guzik, Nat. Photonics **9**, 615 (2015).

[43] C. S. Hamilton, R. Kruse, L. Sansoni, S. Barkhofen, C. Silberhorn, and I. Jex, Phys. Rev. Lett. **119**, 170501 (2017).

[44] C. Weedbrook, S. Pirandola, R. García-Patrón, N. J. Cerf, T. C. Ralph, J. H. Shapiro, and S. Lloyd, Rev. Mod. Phys. **84**, 621 (2012).
[45] R. Kruse, C. S. Hamilton, L. Sansoni, S. Barkhofen, C. Silberhorn, and I. Jex, Phys. Rev. A **100**, 032326 (2019).
[46] W. Roga and M. Takeoka, Sci. Rep. **10**, 14739 (2020).
[47] S. L. Braunstein and P. van Loock, Rev. Mod. Phys. **77**, 513 (2005).
[48] J. Eisert and M. B. Plenio, Int. J. Quantum Inf. **01**, 479 (2003).
[49] A. Ferraro, S. Olivares, and M. Paris, *Gaussian States in Quantum Information*, Napoli Series on Physics and Astrophysics (Bibliopolis, Napoli, Italy, 2005).
[50] F. Duschinsky, Acta Physicochim. URSS **7** (1937).
[51] M. J. Frish *et al.*, Gaussian 98W, Revision A.7, Gaussian, Inc., Pittsburgh, PA, 1998.
[52] A. Serafini, *Quantum Continuous Variables: A Primer of Theoretical Methods* (CRC, Boca Raton, FL, 2017), p. 96.
[53] N. Quesada, L. G. Helt, J. Izaac, J. M. Arrazola, R. Shahrokhshahi, C. R. Myers, and K. K. Sabapathy, Phys. Rev. A **100**, 022341 (2019).
[54] A. Björklund, B. Gupt, and N. Quesada, J. Exp. Algorithmics **24**, 1.11:1 (2019).
[55] R. Kan, J. Multivariate Anal. **99**, 542 (2008).
[56] J. Calsamiglia, R. Muñoz Tapia, L. Masanes, A. Acin, and E. Bagan, Phys. Rev. A **77**, 032311 (2008).
[57] E. Ising, Z. Phys. **31**, 253 (1925).
[58] N. Schuch and J. I. Cirac, Phys. Rev. A **82**, 012314 (2010).
[59] M. Grant and S. Boyd, CVX: Matlab Software for Disciplined Convex Programming, Version 2.1.
[60] S.-X. Zhang, arXiv:1911.04122.
[61] G. I. Orlova and Y. G. Dorfman, Eng. Cyber. **10**, 502 (1972).
[62] F. Hadlock, SIAM J. Comput. **4**, 221 (1975).